NEAR OPTIMUM CONTROL OF A FULL CAR ACTIVE SUSPENSION SYSTEM

Paolo Lino and Bruno Maione
Dipartimento di Elettrotecnica ed Elettronica, Politecnico di Bari, via Re David 200, 70125, Bari, Italy

Keywords: Active suspension, Suspension control, Virtual prototyping, Near-optimum control, AMESim©.

Abstract: In this paper, a near-optimum control strategy applied to a full car model equipped with an active suspension system is presented. The control law is based on a reduced order model obtained by means of a modal aggregation method, achieving a compromise between computational effort in deriving the control law and system performances. To assess the controller performances, a virtual prototype of the suspension system is developed by using AMESim, an advanced fluid-mechanic developing tool. The virtual prototype could be assumed as a reliable model of the real system enabling to perform safer and cheaper tests than using the real system. Simulation results show the effectiveness of the approach.

1 INTRODUCTION

A vehicle suspension system mainly aims to carry the car and its weight, control the vehicle direction of travel, keep the tires in contact with the road, and reduce the effect of shock forces due to road disturbances, braking and entries into curves. Handling and ride comfort can be significantly improved by using active suspension systems instead of passive or semi-active suspensions. More in details, passive suspension systems include spring and dampers characterized by static input-output relationships; semi-active suspensions use dampers with a variable damping coefficient; active suspensions apply a force on car body and wheels by means of an active actuator. The design process of control systems for active and semi-active suspensions is usually carried on by considering quarter car or half car models. The former only represents the vertical motion of the car body, the latter includes pitch or roll motions. Full car models give a more detailed representation of the car dynamics by including vertical displacement, pitch and roll dynamics at the same time. Different approaches to active suspensions control have been investigated by researchers, which are mainly based on fuzzy logic, adaptive control, LQR control and H_∞ control, see (Yoshimura et al., 1997; Yoshimura et al., 1999; Huang and Lin, 2003; Al-Holou et al., 2002; Fialho and Balas, 2002; Alleyene and Hedrick, 1995; Hrovat, 1997) and the references therein.

The main drawback in using lower order models is that interactions between suspensions are neglected, so that the control action cannot compensate angular accelerations or sensibly improve stability. On the other hand, using simplified models makes the controller design easier. In this paper, a compromise between computational effort, detail in representing the system behaviour and controller performances is achieved by applying a near-optimum control strategy to a full car model equipped with an active suspension system. The controller performances are assessed by a virtual prototype of the suspension system. The virtual prototype could be assumed as a reliable model of the real system enabling to perform safer and cheaper tests than using the real system. Moreover, the integration of design and optimization processes of both mechanical and control subsystems are made easier by taking into account mutual interactions (Lino and Maione, 2007), thus reducing the whole design effort.

The proposed design process consists in few steps. Firstly, a 14^{th} order full car analytical model is developed, representing vertical car body and wheels motion, as well as pitch and roll angles dynamics. Then, a reduced order model is derived by applying a modal aggregation technique and used to develop a near-optimum control strategy. Finally, the virtual prototype of suspension system is built to validate the controller performances.

The paper is organized as follows. Sections 2 and 3 describe the full car analytical model and the virtual prototype of suspension system, respectively. The near-optimum control strategy is then introduced in Section 4. Some simulation results concerning the controlled system are shown in Section 5. Finally,

Lino P. and Maione B. (2008).
NEAR OPTIMUM CONTROL OF A FULL CAR ACTIVE SUSPENSION SYSTEM.
In *Proceedings of the Fifth International Conference on Informatics in Control, Automation and Robotics - SPSMC*, pages 46-52
DOI: 10.5220/0001498200460052

Section 6 gives some conclusions.

2 DYNAMICAL MODEL OF THE FULL CAR SUSPENSION SYSTEM

The full car model of a suspension system represents the vehicle as a rigid body with seven degrees of freedom, which originate from translation motion along axes, as well as rotational motions, i.e. pitch and roll motions around center of gravity (COG) (Ikenaga et al., 2000).

With reference to Fig. 1, by setting COG of the car body as origin of axes, the vehicle body dynamics can be described by the following equations:

$$\begin{cases} m_c\ddot{z} = f_{fl} + f_{fr} + f_{rl} + f_{rr} \\ I_{pc}\ddot{\theta} = -f_{fl}l_f + f_{fr}l_f + f_{rl}l_r + f_{rr}l_r \\ I_{rc}\ddot{\phi} = \frac{1}{2}f_{fl}Tr - \frac{1}{2}f_{fr}Tr + \frac{1}{2}f_{rl}Tr + \frac{1}{2}f_{rr}Tr \end{cases} \quad (1)$$

where z is the vertical displacement of car body COG, f_{fl}, f_{fr}, f_{rl}, f_{rr} are the forces applied by front-left, front-right, rear-left, rear-right suspensions on the car body, respectively, θ and ϕ are the pitch and roll angles, respectively, l_f and l_r are the distances from the front and rear axles to car body COG, Tr is the wheels track, m_c is the car body mass, I_{pc} and I_{rc} are the pitch and roll moments of inertia of the car body, respectively.

The force applied to the car body by each suspension can be computed as in the following:

$$\begin{cases} f_i = k_{s,i}(z_{w,i} - z_i) + c_{s,i}(\dot{z}_{w,i} - \dot{z}_i) + f_{A,i} \\ m_{w,i}\ddot{z}_{w,i} = -k_{s,i}(z_{w,i} - z_i) - c_{s,i}(\dot{z}_{w,i} - \dot{z}_i) + \\ \qquad - k_{w,i}(z_{w,i} - z_{r,i}) - f_{A,i} \end{cases} \quad (2)$$

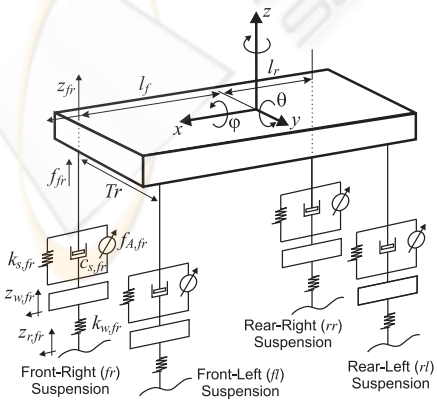

Figure 1: Vertical body model of the full car suspension system.

where subscript $i \in \{fl, fr, rl, rr\}$ characterizes the four suspensions, $z_{w,i}$ and z_i are the vertical displacements of the wheel COG and car body corner, respectively, $m_{w,i}$ is the wheel mass, $k_{s,i}$ and $c_{s,i}$ are the stiffness and damping factor of the suspension, respectively, $k_{w,i}$ is the wheel stiffness, and $f_{A,i}$ is the active force applied by the controlled actuator.

The following equations express the vertical displacement of car body corners in terms of z, θ and ϕ:

$$\begin{aligned} z_{fl} &= z + \frac{1}{2}Tr\cdot\sin\phi - l_f\sin\theta \approx z + \frac{1}{2}Tr\cdot\phi - l_f\theta \\ z_{fr} &= z - \frac{1}{2}Tr\cdot\sin\phi - l_f\sin\theta \approx z - \frac{1}{2}Tr\cdot\phi - l_f\theta \\ z_{rl} &= z + \frac{1}{2}Tr\cdot\sin\phi + l_r\sin\theta \approx z + \frac{1}{2}Tr\cdot\phi + l_r\theta \\ z_{rr} &= z - \frac{1}{2}Tr\cdot\sin\phi + l_r\sin\theta \approx z - \frac{1}{2}Tr\cdot\phi + l_r\theta \end{aligned} \quad (3)$$

where the approximations hold for small variations of pitch and roll angles. Combining equations (1), (2) and (3) results in a system of differential equations of the form:

$$\begin{cases} m_c\ddot{z}_c = f_1(z_c, \dot{z}_c, z_{w,i}, \dot{z}_{w,i}, \phi, \dot{\phi}, \theta, \dot{\theta}, f_{A,i}) \\ I_{pc}\ddot{\theta} = f_2(z_c, \dot{z}_c, z_{w,i}, \dot{z}_{w,i}, \phi, \dot{\phi}, \theta, \dot{\theta}, f_{A,i}) \\ I_{rc}\ddot{\phi} = f_3(z_c, \dot{z}_c, z_{w,i}, \dot{z}_{w,i}, \phi, \dot{\phi}, \theta, \dot{\theta}, f_{A,i}) \end{cases} \quad (4)$$

Equations (4), together with those of wheels vertical displacements:

$$m_r\ddot{z}_{w,i} = f_{4,i}(z_c, \dot{z}_c, z_{w,i}, \dot{z}_{w,i}, z_{r,i}, \theta, \dot{\theta}, \phi, \dot{\phi}, f_{A,i}) \quad (5)$$

represent the full car dynamics under the action of road disturbances and actuation forces. The design of a control law can be simplified by putting equations (4) and (5) in a state space form:

$$\dot{\mathbf{x}} = \mathbf{A}\mathbf{x} + \mathbf{B}\mathbf{f} + \mathbf{H}\mathbf{d}, \quad (6)$$

where $\mathbf{f} = [f_{A,fl}, f_{A,fr}, f_{A,rl}, f_{A,rr}]^T$ is the vector of actuation forces, $\mathbf{d} = [z_{r,fl}, z_{r,fr}, z_{r,rl}, z_{r,rr}]^T$ is the vector of road disturbances, and $\mathbf{x}$ is the state vector, composed of vertical displacements, pitch and roll angles and its derivatives.

A more accurate model of the suspension system includes the actuators dynamics. In this paper, the hydraulic actuator described in (Rajamani and Hedrick, 1995) is considered. It consists of a cylinder with a moving piston pushed by the pressure difference on its upper and lower surfaces (Fig. 2).

The pressure difference is regulated by an electronic valve driven by the control system. Under the assumption of a negligible piston inertia with respect to high hydraulic forces, the actuation force is given by:

$$f_{A,i} = -A_{y,i}(\dot{z}_{c,i} - \dot{z}_{w,i}) + u_i, \quad (7)$$

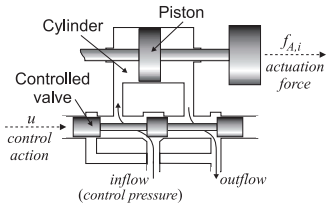

Figure 2: Hydraulic actuator for active suspensions.

where u is a linear function of the control pressure set by acting on the electronic valve, and $A_{y,i}$ is a constant parameter depending on the system geometry and working fluid characteristics. By suitably introducing an $\mathbf{E}$ matrix, the system state space model becomes:

$$\dot{\mathbf{x}} = (\mathbf{A} + \mathbf{BE})\mathbf{x} + \mathbf{Bu} + \mathbf{Hd}, \tag{8}$$

where $\mathbf{u}$ is the vector of control inputs u_i.

3 VIRTUAL PROTOTYPE OF THE SUSPENSION SYSTEM

As virtual environment for design integration, we use AMESim© (Advanced Modelling Environment for Simulation): a simulation tool, which is oriented to lumped parameter modelling of components from different physical domains, interconnected by ports enlightening the energy exchanges between element and element and between an element and its environment. It also guarantees a flexible architecture, capable of including new components defined by the users (IMAGINE S.A., 2004).

The AMESim virtual prototype (Fig. 3) used to evaluate the controller performances has been developed by employing the AMESim-Simulink interface in Co-simulation mode: each suspension-wheel subsystem is modelled within the AMESim environment; the car body dynamical equations (1) are solved using MATLAB. AMESim and Simulink cooperate by integrating the relevant portions of models.

The main components of each suspension-wheel subsystem are the *Mass block with stiction and coulomb friction and end stops*, which computes the wheel dynamics through the Newtons second law of motion, the *Mechanical spring and dumper* computing the elastic and damping forces of suspensions and wheels depending on nonlinear stiffness and damping coefficients, the *Piston with moving body*, representing the actuator hydraulic circuit dynamics and computing the pressure forces acting upon the upper and lower piston surfaces, and the *3 positions hydraulic control valve* modelling the electro-hydraulic circuit driving the actuator.

The pressure dynamics inside cylinders are computed as a function of intake and outtake flows Q_{in}, Q_{out}, as well as of volume changes due to mechanical part motions, according to the following equation:

$$\frac{dP}{dt} = \frac{K_f}{v}\left(\rho\frac{dv}{dt} - Q_{in} + Q_{out}\right), \tag{9}$$

where P and ρ are the working fluid pressure and density, respectively, and v is the taken up volume. Q_{in} and Q_{out} can be calculated by applying the energy conservation law, which gives, for a generic Q:

$$Q = c_D(\rho,\eta)A\rho\sqrt{\frac{2|\Delta P|}{\rho}}sgn(\Delta P), \tag{10}$$

where ΔP is the working fluid pressure difference across the flow section A; $sgn(\Delta P)$ is the sign function affecting the flow direction; the discharge coefficient c_D accounts for nonuniform flow rates and flow process non-isentropicity, depending on fluid density ρ and cinematic viscosity η. Finally, the *3 positions hydraulic control valve* block models the controlled valve as a second order spring-damp linear system.

To take into account the influence of inertia on pitch and roll dynamics during brakes and entries into a curve, the following equations are included in the model:

$$\begin{cases} I_{PC}\theta = m_c h_{cg}\ddot{x} \\ I_{PC}\phi = m_c h_{cg}\ddot{y} \end{cases}, \tag{11}$$

where h_{cg} is the distance from the contact point between wheel and suspension to car body COG, and $\ddot{x}$ and $\ddot{y}$ are the COG accelerations along x and y axes, respectively.

4 THE NEAR-OPTIMUM CONTROL STRATEGY

Given a system described by the state space equations:

$$\begin{aligned} &\dot{\mathbf{x}}(t) = \mathbf{Ax}(t) + \mathbf{Bu}(t), \quad \mathbf{x}(0) = \mathbf{x}_0, \\ &\mathbf{y}(t) = \mathbf{Dx}(t) \end{aligned} \tag{12}$$

and a quadratic cost function:

$$J = \int_0^\infty \left(\mathbf{x}(t)^\mathbf{T}\mathbf{Q}\mathbf{x}(t) + \mathbf{u}(t)^\mathbf{T}\mathbf{R}\mathbf{u}(t)\right)dt, \tag{13}$$

being $\mathbf{Q}$ and $\mathbf{R}$ two positive semi-definite matrices, it is well known that the Linear-Quadratic-Regulator (LQR) problem consists in finding an input vector $\mathbf{u}^*(t) = -\mathbf{Kx}(t)$ minimizing the cost function J via state-feedback (Dorato et al., 2000). The state feedback matrix $\mathbf{K}$ can be computed as:

$$\mathbf{K} = \mathbf{R}^{-1}\mathbf{B}^\mathbf{T}\mathbf{P}, \tag{14}$$

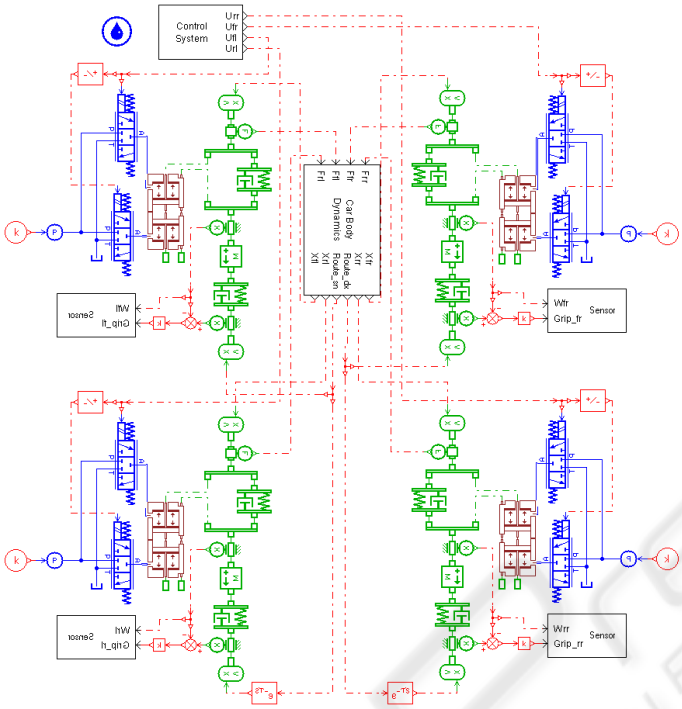

Figure 3: AMESim virtual prototype of the full car suspension system.

where $\mathbf{P}$ is the solution of the following matrix Riccati equation:

$$\mathbf{A}^{\mathbf{T}}\mathbf{P}+\mathbf{P}\mathbf{A}-\mathbf{P}\mathbf{B}\mathbf{R}^{-1}\mathbf{B}^{\mathbf{T}}\mathbf{P}+\mathbf{Q}=0. \quad (15)$$

$\mathbf{Q}$ and $\mathbf{R}$ matrices can be considered as weights on state and control input, respectively, and affect the value assumed by elements of matrix $\mathbf{K}$. The Riccati equation complexity directly depends on the system order and its solution requests $n(n+1)/2$ operations. For a high order system it calls for a large computational effort, which could not be sustainable for on line calculations; a solution consists in adopting large scale system techniques to reduce problem complexity and make the application of optimal control theory easier (Jamshidi, 1983). These approaches, which are based on reduction of order, perturbation of parameters, decomposition of structure, hierarchical interaction or decentralization of control, lead to near optimality of system performance.

In this paper, the aggregation method based on the *modal approach* is applied to reduce the model order (Jamshidi, 1983). More in details, it neglects the effect of non dominant modes to obtain a system of *aggregated states* ζ:

$$\begin{aligned}\dot{\zeta}(t)&=\mathbf{F}\zeta(t)+\mathbf{G}\mathbf{u}(t),\zeta(0)=\zeta_0\\ \dot{\mathbf{y}}(t)&=\mathbf{L}\zeta(t)\end{aligned} \quad (16)$$

by using a transformation matrix $\mathbf{C}$:

$$\zeta(t)=\mathbf{C}\mathbf{x}(t),\quad \zeta(0)=\mathbf{C}\mathbf{x}(0). \quad (17)$$

The reduced order model matches the full order model dynamics if the *dynamic exactness* condition holds:

$$\begin{aligned}\mathbf{F}\mathbf{C}&=\mathbf{C}\mathbf{A}\\ \mathbf{G}&=\mathbf{C}\mathbf{B}\\ \mathbf{L}\mathbf{C}&=\mathbf{D}.\end{aligned} \quad (18)$$

By defining an error vector $\mathbf{e}(t)=\zeta(t)-\mathbf{C}\mathbf{x}(t)$, its dynamics is described by the equation $\dot{\mathbf{e}}=\mathbf{F}\mathbf{e}+(\mathbf{F}\mathbf{C}-\mathbf{C}\mathbf{A})\mathbf{x}+(\mathbf{G}-\mathbf{C}\mathbf{B})\mathbf{u}$, which reduces to $\dot{\mathbf{e}}=\mathbf{F}\mathbf{e}$ if conditions (18) hold. Provided that $\mathbf{F}$ is a positive definite matrix, error reduces to 0 even for $e(0)\neq 0$.

To derive the aggregation matrix $\mathbf{C}$, the modal approach exploits the system modal matrix $\mathbf{M}$, whose elements are the eigenvectors of state matrix $\mathbf{A}$. Hence, if arranging columns of matrix $\mathbf{M}$ by starting from eigenvectors related to slowest dynamics, the reduced order system matrices can be obtained using the following relationships:

$$\begin{aligned}\mathbf{F}&=\mathbf{M}_l\mathbf{S}\Lambda\mathbf{S}^{\mathbf{T}}\mathbf{M}_l^{-1}\\ \mathbf{C}&=\mathbf{M}_l\mathbf{S}\mathbf{M}^{-1}\\ \mathbf{G}&=\mathbf{C}\mathbf{B}\\ \mathbf{L}&\approx\mathbf{D}\mathbf{C}^{+}\end{aligned} \quad (19)$$

where $\mathbf{M}_l$ is the nonsingular leading principal minor of matrix $\mathbf{M}$ of order l, $\mathbf{S}=[\mathbf{I}_l \quad 0]$, being $\mathbf{I}_l$ the Identity matrix, Λ is the Jordan matrix of $\mathbf{A}$, and $\mathbf{C}^{+}$ is the pseudo-inverse of $\mathbf{C}$.

Considering the reduced order system, the Riccati equation becomes:

$$\mathbf{F}^{\mathbf{T}}\mathbf{P}_a + \mathbf{P}_{\mathbf{F}} - \mathbf{P}_a\mathbf{G}\mathbf{R}^{-1}\mathbf{G}^{\mathbf{T}}\mathbf{P}_a + \mathbf{Q}_a = 0, \quad (20)$$

so that the following control action is obtained:

$$\begin{aligned}\mathbf{u}_a(t) &= -\mathbf{R}^{-1}\mathbf{G}^{\mathbf{T}}\mathbf{P}_a\zeta(t) = -\mathbf{R}^{-1}\mathbf{G}^{\mathbf{T}}\mathbf{P}_a\mathbf{C}\mathbf{x}(t) \\ &= -\mathbf{K}_a\mathbf{x}(t)\end{aligned} \quad (21)$$

By pre- and post- multiplying eq. (20) by $\mathbf{C}^{\mathbf{T}}$ and $\mathbf{C}$, respectively, and considering the aggregation conditions, it is straightforward to obtain:

$$\begin{aligned}&\mathbf{A}^T(\mathbf{C}^{\mathbf{T}}\mathbf{P}_a\mathbf{C}) + (\mathbf{C}^{\mathbf{T}}\mathbf{P}_a\mathbf{C})\mathbf{A} + \\ &-(\mathbf{C}^{\mathbf{T}}\mathbf{P}_a\mathbf{C})\mathbf{B}\mathbf{R}^{-1}\mathbf{B}^{\mathbf{T}}(\mathbf{C}^{\mathbf{T}}\mathbf{P}_a\mathbf{C}) + \mathbf{C}^{\mathbf{T}}\mathbf{Q}_a\mathbf{C} = 0.\end{aligned} \quad (22)$$

Equations (15) and (22) coincide provided that the following positions hold:

$$\begin{aligned}\mathbf{P} &= \mathbf{C}^{\mathbf{T}}\mathbf{P}_a\mathbf{C}, \\ \mathbf{Q} &= \mathbf{C}^{\mathbf{T}}\mathbf{Q}_a\mathbf{C}.\end{aligned} \quad (23)$$

Hence, the $\mathbf{Q}_a$ matrix can be obtained as:

$$\mathbf{Q}_a = (\mathbf{C}\mathbf{C}^{\mathbf{T}})^{-1}\mathbf{C}\mathbf{Q}\mathbf{C}^{\mathbf{T}}(\mathbf{C}\mathbf{C}^{\mathbf{T}})^{-1}. \quad (24)$$

Finally, $\mathbf{K}_a$ matrix is obtained from $\mathbf{F}$, $\mathbf{G}$, $\mathbf{Q}_a$ and $\mathbf{R}$ matrices.

In this paper, a 6^{th} order aggregated model is derived from the full order suspension system and used to derive the control law.

5 SIMULATION RESULTS

To evaluate the controller performances, a set of tests is performed on the virtual prototype by applying different road profiles. In particular, the following benchmarks used in industrial practice are considered (Canale et al., 2006):

- *Sine wave hole* profile: a sine profile hole with 0.03 m of amplitude and 6 m of width; for the sake of brevity, only 30 and 90 Km/h car speeds are considered in this paper;
- *Short back* profile: a positive step of road profile with 0.02 m of amplitude and 0.5 m of width, with a travelling speed of 30 Km/h;
- *Drain well* profile: a negative step variation of road profile with 0.05 m of amplitude and 0.6 m of width, with a traveling speed of 30 km/h.

Moreover, the system response in case of entry in a curve or braking is analysed. The proposed controller performances have been compared with those obtained by using an active decoupled controller (Ikenaga et al., 2000) and an LQR controller based on the full order model. In particular, the control scheme proposed in (Ikenaga et al., 2000) includes a ride control loop, for road disturbances rejection, and an attitude control loop, for roll, pitch and vertical dynamics regulation. To former includes an active filtering feedback, the latter is based on a sky-hook control strategy. A decoupling is performed to deal with the under-actuation problem.

Figure 4 shows pitch and vertical displacement dynamics when applying the sine wave hole road profile. Since the road disturbance is symmetrically applied to left and right wheels, the roll dynamics is negligible and not displayed.

It is evident that the LQR controller guarantees better performances than the near-optimum and the decoupled controllers, in terms of overshoot and settling time. Nevertheless, the near optimum controller allows acceptable pitch angle and vertical displacement dynamics, improving the results obtained with the decoupled controller.

In Figure 5, the *drain well* and the *short back* disturbances are only applied to left wheels, so that the roll angle dynamics is excited. Simulation results show that the LQR controller still guarantees a better system behaviour for all conditions thanks to a prompt control action, while the near-optimum controller improves results obtained with the decoupled controller.

Finally, Figure 6 displays the effect of sudden longitudinal and lateral accelerations determined by braking (Fig. 6(a)), and entry into a curve (Fig. 6(b)), which independently affect the pitch dynamics and the roll dynamics, respectively.

In the former case, the near-optimum and the LQR controllers show similar performances; in the latter case, the near-optimum controller cannot reduce significantly the roll angle overshoot. In general, the decoupled controller cannot guarantee fast transients due to actuator saturation; the near optimum and LQR controller can suitably restrain the control action thanks to a suitable choice of the performance index weights. To sum up, the near optimum controller represents a compromise in terms of system performances and complexity, while the LQR controller always shows the best performances.

6 CONCLUSIONS

In this paper, a near-optimum control strategy applied to a full-car active suspension system has been proposed. The design process relies on the use of a high order analytical model, from which an aggregated low order model is derived, and of a virtual prototype developed by using the AMESim simulation package.

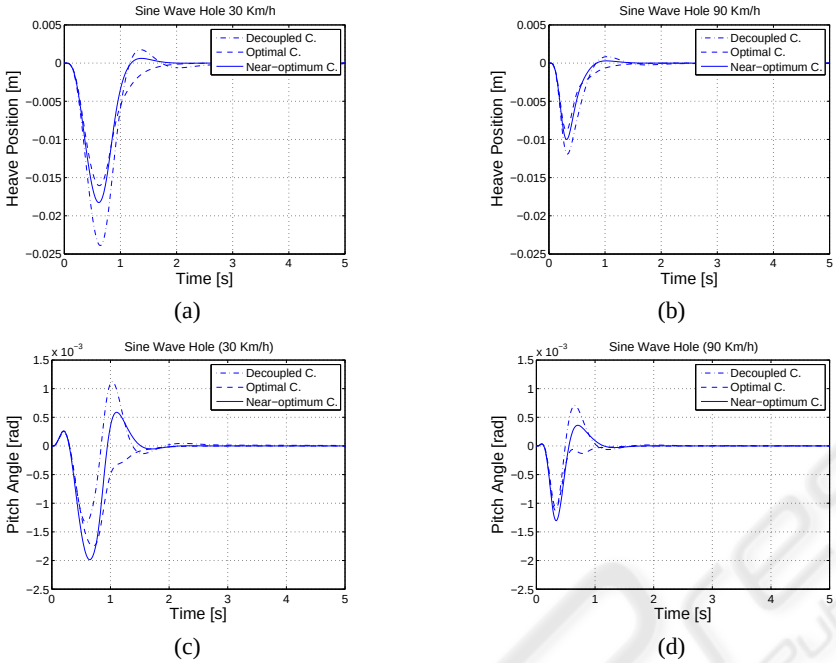

Figure 4: Vertical displacement (a)-(b) and Pitch angle (c)-(d) dynamics for a sine wave hole road profile ran at 30 km/h and 90 km/h, respectively.

The virtual prototype represents a reliable benchmark for evaluating the controller performances before the implementation on the real system. Moreover, it can be used for the integrated design of both mechanical and control subsystems at the same time. As simulation experiments have shown, the proposed controller provides good performances, despite the low computational effort required.

REFERENCES

Al-Holou, N., Lahdhiri, T., Joo, D., Weaver, J., and Al-Abbas, F. (2002). Sliding mode neural network inference fuzzy logic control for active suspension systems. *IEEE Transactions on Fuzzy Systems*, 10(2):234–246.

Alleyene, A. and Hedrick, J. (1995). Nonlinear adaptive control of active suspensions. *IEEE Transactions on Control Systems Technology*, 3(1):94–101.

Canale, M., Milanese, M., and Novara, C. (2006). Semi-Active Suspension Control Using 'Fast' Model-Predictive Techniques. *IEEE Transactions on Control Systems Technology*, 14(6):1034–1046.

Dorato, P., Abdallah, C., and Cerone, V. (2000). *Linear Quadratic Control: An Introduction*. Krieger Publishing Company, Melbourne.

Fialho, I. and Balas, G. (2002). Road adaptive active suspension design using linear parameter-varying gain-scheduling. *IEEE Transactions on Control Systems Technology*, 10(1):43–54.

Hrovat, D. (1997). Survey of Advanced Suspension Developments and Related Optimal Control Applications. *Automatica*, 33(10):1781–1817.

Huang, S. and Lin, W. (2003). Adaptive fuzzy controller with sliding surface for vehicle suspension control. *IEEE Transactions on Fuzzy Systems*, 11(4):550–559.

Ikenaga, S., Lewis, F., Campos, J., and Davis, L. (2000). Active suspension control of ground vehicle based on a full-vehicle model. In *ACC 2000, Proceedings of the 2000 American Control Conference*.

Jamshidi, M. (1983). *Large-Scale Systems: Modeling and Control*. Elsevier Science Ltd, Amsterdam.

Lino, P. and Maione, B. (2007). Integrated design of a mechatronic system - the pressure control in common rails. In *ICINCO 2007, Proceedings of the Fourth International Conference on Informatics in Control, Automation and Robotics*, Angers, France.

Rajamani, R. and Hedrick, J. (1995). Adaptiver Observers for Active Automotive Suspensions: Theory and Experiment. *IEEE Transactions on Control Systems Technology*, 3(1):86–93.

IMAGINE S.A. (2004). *AMESim User Manual v4.2*. Roanne, France.

Yoshimura, T., Isari, Y., Li, Q., and Hino, J. (1997). Active suspension of motor coaches using skyhook damper and fuzzy logic control. *Control Engineering Practice*, 5(2):175–184.

Yoshimura, T., Nakaminami, K., Kurimoto, M., and Hino, J. (1999). Active suspension of passenger cars using linear and fuzzy-logic controls. *Control Engineering Practice*, (7):41–47.

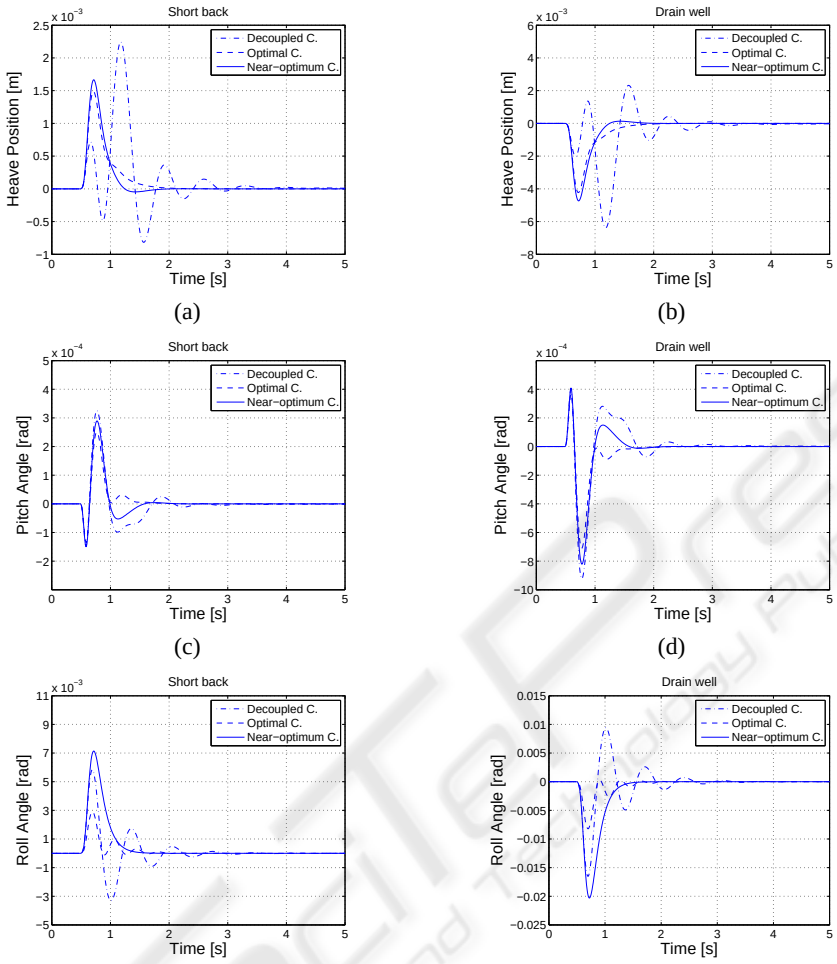

Figure 5: Vertical displacement, pitch angle and roll angle dynamics when applying *short back* and *drain well* road disturbances; (a)-(c)-(e) *short back* disturbance applied ; (b)-(d)-(f) drain well disturbance applied.

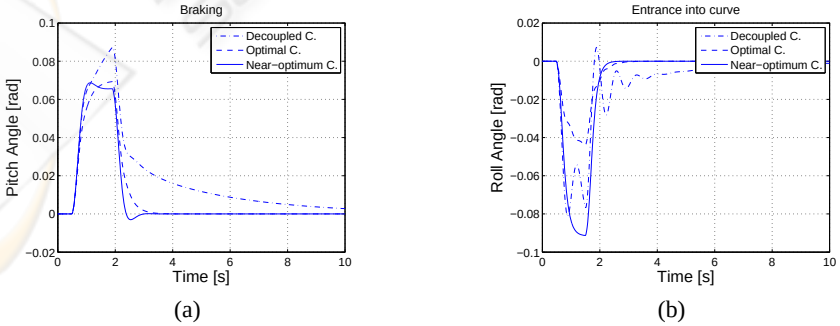

Figure 6: Pitch angle (a) and roll angle (b) dynamics in case of braking and entry into a curve, respectively.